Physisorption of N_2, O_2, and CO on Fully Oxidized TiO_2(110)

Zdenek Dohnálek,*,† Jooho Kim,† Oleksandr Bondarchuk,‡ J. Mike White,†,‡ and Bruce D. Kay*,†

Pacific Northwest National Laboratory, Fundamental Sciences Directorate and Institute for Interfacial Catalysis, Richland, Washington 99352, and Center for Materials Chemistry, Texas Materials Institute, University of Texas, Austin, Texas 78712

Received: November 9, 2005; In Final Form: January 21, 2006

Physisorption of N_2, O_2, and CO was studied on fully oxidized TiO_2(110) using beam reflection and temperature-programmed desorption (TPD) techniques. Sticking coefficients for all three molecules are nearly equal (0.75 ± 0.05) and approximately independent of coverage suggesting that adsorption occurs via a precursor-mediated mechanism. Excluding multilayer coverages, the TPD spectra for all three adsorbates exhibit three distinct coverage regimes that can be interpreted in accord with previous theoretical studies of N_2 adsorption. At low coverages (0−0.5 N_2/Ti^{4+}), N_2 molecules bind head-on to five-coordinated Ti^{4+} ions. The adsorption occurs preferentially on the Ti^{4+} sites that do not have neighboring adsorbates. This arrangement minimizes the repulsive interactions between the adsorbed molecules along the Ti^{4+} rows resulting in a relatively small shift of the TPD peak (105 → 90 K) with increasing coverage. At higher N_2 coverages (0.5−1.0 N_2/Ti^{4+}) the nearest-neighbor Ti^{4+} sites become occupied. The close proximity of the adsorbates results in strong repulsion thus giving rise to a significant shift of the TPD leading edges (90 → 45 K) with increasing coverage. For $N_2/Ti^{4+} > 1$, an additional low-temperature peak (∼43 K) is present and is ascribed to N_2 adsorption on bridge-bonded oxygen rows. The results for O_2 and CO are qualitatively similar. The repulsive adsorbate−adsorbate interactions are largest for CO, most likely due to alignment of CO dipole moments. The coverage-dependent binding energies of O_2, N_2, and CO are determined by inverting TPD profiles.

I. Introduction

Among oxides, the rutile TiO_2(110) surface has become one of the most extensively studied.[1] The wide-ranging importance of TiO_2 in heterogeneous catalysis, photocatalysis, sensor applications, and solar cell H_2 production is well recognized and serves as an important driving force for fundamental studies.[1] Despite the fact that TiO_2 is a technologically relevant material, the interactions of well-characterized TiO_2 surfaces with simple molecules (e.g., CO, N_2, and O_2) that participate as reagents or products in a number of catalytic reactions on TiO_2 are not well understood. Surprisingly, even basic parameters characterizing the adsorption/desorption processes, such as binding energies and sticking probabilities, are not known. The primary reason for the absence of such data is the weak binding of these adsorbates which necessitates carrying the experiments out at very low temperatures (∼30 K). The experimental difficulties associated with mounting and cooling of oxide single crystals are well recognized in the surface science community and are largely responsible for the lack of data at these cryogenic temperatures.

Recently it has been demonstrated that the catalytic oxidation of CO on Au nanoclusters supported on TiO_2(110) can occur at very low temperatures.[2,3] At present, our understanding of this important catalytic reaction is incomplete. Clearly, the adsorption and desorption of species such as CO and O_2 on various surface sites of the TiO_2(110) surface play an important role in the CO oxidation reaction.[4] To date only a few experimental studies have examined CO adsorption on well-characterized TiO_2(110).[5,6] Limited by the lowest temperature (105 K) reachable, the first study[5] measured temperature-programmed desorption (TPD) spectra for CO coverages no higher than 2.1×10^{14} CO/cm^2. This coverage is 40% of the number of exposed five-fold-coordinated Ti^{4+} (hereafter called Ti^{4+}) sites on TiO_2(110). The TPD spectra in this CO coverage range exhibited a single peak with the desorption maximum decreasing from 150 to 135 K with increasing CO coverage. A zero-coverage value for the CO desorption energy was estimated to be 42 kJ/mol using a preexponential factor of 1×10^{14} s^{-1}. The second study[6] performed at a base temperature of ∼80 K determined the CO sticking coefficient as a function of coverage, impact energy, adsorption temperature, and the angle of incidence along [001] and [1$\bar{1}$0] azimuths. For small impact energies ($E_I < 0.5$ eV), the initial sticking probability decreases exponentially with increasing E_I and obeys total energy scaling as previously observed on MgO(100).[7]

Adsorption in UHV of both O_2 and N_2 on fully oxidized TiO_2-(110) is also limited if temperatures below 100 K are not reachable. Prior studies of O_2 adsorption are limited to partially reduced TiO_2(110) surfaces where a small amount of O_2 desorption is observed at ∼410 K.[8,9]

The adsorption of CO on TiO_2(110) has been examined theoretically by a number of groups using different approaches.[10−15] The calculated CO binding energies vary widely and depend strongly on the computational method employed. In general, CO is found to adsorb preferentially upright with the C atom end of the molecule bound on top of the five-fold-coordinated Ti^{4+} site. The calculated binding

* Corresponding authors. E-mail: Zdenek.Dohnalek@pnl.gov. (Z.D.); Bruce.Kay@pnl.gov (B.D.K.).
† Pacific Northwest National Laboratory.
‡ University of Texas, Austin.

10.1021/jp0564905 CCC: $33.50
Published on Web 03/08/2006

energy for this configuration varies from 23 to 77 kJ/mol.[10−15] When the O end is bound to Ti^{4+}, adsorption is weak (2.6−11.4 kJ/mol).[12]

Recent theoretical studies of N_2 adsorption on TiO_2(110), carried out by Rittner and co-workers,[16−18] are germane to our experimental results. These studies employ ab initio quantum mechanical cluster calculations to determine N_2 binding energies[16,17] which are used to construct a N_2/TiO_2(110) potential energy surface (PES).[17] The N_2 molecule is predicted to adsorb upright on top of the Ti^{4+} sites with binding energies of 37 and 46 kJ/mol for H-terminated and point-charge-embedded Ti_9O_{18} clusters, respectively. The resulting PES is used in Kinetic Monte Carlo (KMC) simulations to calculate N_2 adsorption as a function of N_2 pressure at 77 K.[18] One of the outcomes of the KMC simulations is the fact that after saturation of the Ti^{4+} sites with N_2 (5.2×10^{14} N_2/cm^2), an additional 2.6×10^{14} cm^2 of weakly bound N_2 can be adsorbed on top of the bridge-bonded oxygen (BBO) rows. Relative to the Ti^{4+} sites/cm^2, this saturation coverage is 1.5 ML; 1 ML of N_2 is bound to the Ti^{4+} sites in tilted orientation, while 0.5 ML is bound to the BBOs with the N≡N axis parallel to the surface and perpendicular to the BBO rows.

While molecular and dissociative adsorption of O_2 on BBO vacancies of TiO_2(110) has been examined theoretically,[19−22] we are not aware of any theoretical study dealing with O_2 adsorption on fully oxidized TiO_2(110).

In this article, we present a detailed experimental study of the physisorption of N_2, O_2, and CO on the fully oxidized TiO_2-(110) surface. These experiments were performed at temperatures as low as ∼32 K, thereby enabling adsorption of these weakly bound species. All three molecules exhibit qualitatively similar behavior. At low coverage (≤0.5 molecules/Ti^{4+}) the TPD spectra exhibit a desorption peak that shifts slightly to lower temperature with increasing coverage. On the basis of the aforementioned calculations[16−18] these adsorbates are ascribed to adsorption at nonadjacent Ti^{4+}. At intermediate coverages (0.5−1 molecules/Ti^{4+}), the TPD spectra exhibit a dramatic shift to lower temperature with increasing coverage. The shift is attributed to increasingly strong repulsive adsorbate−adsorbate interactions as the remaining Ti^{4+} sites are filled. At even higher coverages (1.0−1.5 molecules/Ti^{4+}) a relatively sharp low-temperature peak emerges in the TPD spectra and is attributed to weak molecular adsorption on the BBO rows. For even higher doses, multilayer coverages begin to appear. The initial sticking coefficients of CO, N_2, and O_2 on clean TiO_2-(110) are equal to 0.80, 0.75, and 0.72, respectively, with an absolute uncertainty of ±0.05. The sticking coefficients are nearly coverage independent indicating precursor-mediated adsorption. These experiments on fully oxidized TiO_2(110) provide the necessary reference point for the future studies of partially reduced TiO_2(110) surfaces where the binding of simple adsorbates on BBO vacancy defects can be explored.

II. Experimental Section

The experiments were conducted in an ultrahigh vacuum (UHV) molecular beam−surface scattering apparatus having a base pressure of $\sim 1 \times 10^{-10}$ torr. The TiO_2(110) sample ($10 \times 10 \times 1$ mm^3, Princeton Scientific) was mounted using a 1.25 cm diameter Mo holder composed of a 1 mm thick base plate with a square (10×10 mm^2) recession 0.25 mm deep machined into it. The TiO_2(110) single-crystal sample is seated in this recession and covered by a 0.1 mm thick retaining ring having an 8 mm clear opening in its center. The Mo retaining ring and the captured sample are secured to the base plate by four Mo screws. Collimated molecular beams enable dosing only the exposed portion of the TiO_2(110) sample. This configuration avoids adsorption on any of the metallic components of the sample holder. The temperature of the substrate was measured using a W−5%Re/W−26%Re thermocouple cemented to the back of the sample using a ZrO_2-based ceramic adhesive (Aremco Ultra-Temp 516). The thermocouple leads were passed through a small hole machined in the center of the Mo base plate. An absolute temperature calibration (±2 K) was performed by adding a small offset to the thermocouple thermoelectric voltage to match the known multilayer desorption temperatures of various gases (Kr ∼44 K, Xe ∼62 K, and H_2O ∼165 K).[23] In this configuration the TiO_2 sample could be cooled to ∼32 K and heated to ∼1200 K. Cooling from 900 to 32 K took ∼10 min. The TiO_2(110) was cleaned using a repeated sequence of Ne sputtering at 850 K in a background of O_2 (2×10^{-7} torr) followed by annealing in vacuum at 900 K to remove mainly calcium, potassium, and carbon contamination. Approximately six sputter−anneal cycles were employed before acquiring the data presented in this study with the total UHV annealing time at 900 K of less than 1 h. The surface purity and order of the TiO_2(110) substrate were checked using Auger electron spectroscopy (AES) and low-energy electron diffraction (LEED), respectively.

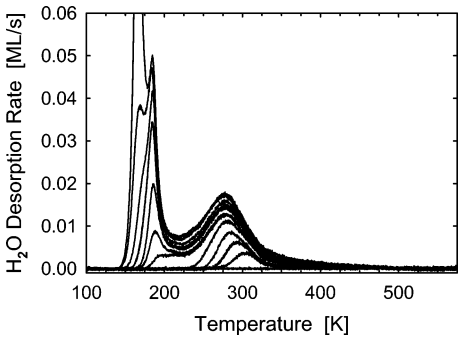

Figure 1. H_2O TPD spectra for various initial H_2O coverages (0−4 ML) on TiO_2(110). H_2O was adsorbed at 32 K, and the sample was heated linearly at a rate of 1 K/s. Here, 1 ML coverage is defined as a saturation coverage of Ti^{4+} sites.

The TiO_2(110) substrate used in this study was only slightly reduced as evidenced by its light-blue color and the absence of a high-temperature H_2O desorption feature (∼490 K) in the TPD. It has been established previously that water dissociates on BBO surface vacancies on TiO_2(110)[24−29] and desorbs recombinatively around 490 K.[25−28] To assess the concentration of BBO surface vacancies on our sample we show coverage-dependent TPD from H_2O adsorbed at 35 K on TiO_2(110) in Figure 1. The H_2O TPD spectrum exhibits three desorption peaks; the first peak at 270−300 K represents desorption from Ti^{4+} sites, the second peak at 185 K corresponds to desorption from BBO sites, and the third peak at 165 K is due to H_2O multilayer desorption. These TPD features are in agreement with previous studies.[24−29] The lack of an observable water desorption feature at ∼490 K clearly indicates that the BBO vacancy concentration on our sample is much smaller than ∼5% which would be easily detectable in our TPD setup.

Neat gases (liquid N_2 boil-off, CO Air Liquide, 99.99%, O_2 NorLab, 99.994%) were dosed using a 300 K, supersonic molecular beam directed normal to the TiO_2(110) surface. The molecular beam was produced by expanding ∼50 torr of gas through a 100 μm diameter circular orifice. This mild supersonic expansion produces beams with kinetic energies between $^5/_2RT$ (6.2 kJ/mol) and $^7/_2RT$ (8.7 kJ/mol). We did not characterize the velocity distribution of these beams in this study. The

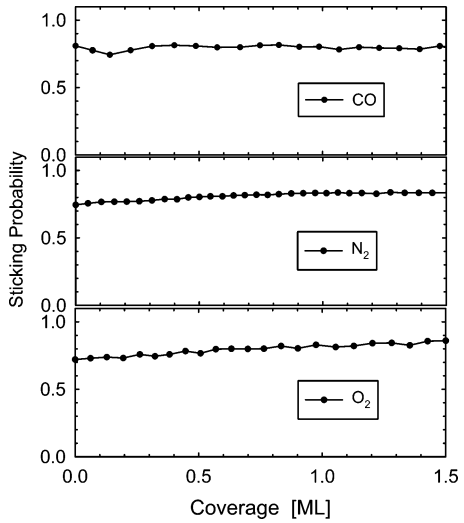

Figure 2. Sticking coefficients vs relative coverages of CO, N_2, and O_2 on TiO_2(110). The coverage axis is calculated from TPD peak areas with 1.5 ML (Figure 8) defined as the maximum area that includes no multilayer contribution (see text). The sample temperature was 32 K. The absolute uncertainty in these values is ±0.05.

adsorption kinetics were monitored using the beam reflection technique of King and Wells[30] and were analyzed using procedures described in detail in our previous publications.[7,31] The desorption kinetics of N_2, O_2, and CO were studied using TPD taken in a line-of-sight arrangement with a quadrupole mass spectrometer. At the beginning of each day the sample was flashed to 900 K to produce a clean sample as evidenced by water TPD and AES. Additionally, the sample was flashed to 600 K between subsequent adsorbate doses. All TPD spectra were acquired using a linear temperature ramp rate of 1 K/s. All adsorbate coverages are defined relative to the area under the desorption curve of a saturated state which we define to be 1.5 ML relative to the Ti^{4+} sites (5.2×10^{14} cm^{-2}). Absolute coverages (molecules/cm^2) determined using a calibrated flux molecular beam[7] and the coverage-dependent sticking probabilities measured in this study agreed with this saturation coverage (±5%) for all three molecules.

III. Results and Discussion

III.A. Sticking Coefficient Measurements. We used the beam reflection technique of King and Wells[30] to measure the sticking coefficients of N_2, O_2, and CO on TiO_2(110) as a function of coverage ($\theta \leq 1.5$ ML (7.8×10^{14} molecules/cm^2)) at normal angle of incidence. Our base temperature of 32 K does not allow us to adsorb multilayers of N_2, O_2, or CO. An example of the raw data for our experimental setup as well as the details of the procedure employed to extract the coverage-dependent sticking coefficients are described in our study of CO on MgO(100).[7]

For all three adsorbates, Figure 2, the initial sticking coefficient is high ($S_0 \cong 0.75 \pm 0.05$) and increases only very slightly with increasing coverage ($S_{1.5ML} \cong 0.80 \pm 0.05$) in good agreement with the $S_0 = 0.85$ for CO/TiO_2(110) reported previously.[6] The large and nearly coverage-independent sticking probabilities observed for N_2, O_2, and CO on TiO_2(110) indicate that energy transfer to the TiO_2 lattice is efficient and that adsorption occurs via a precursor-mediated mechanism. In precursor-mediated adsorption, the molecule traps efficiently on both bare and adsorbate-occupied sites. Molecules which initially trap on occupied adsorption sites readily migrate to, and adsorb at, nearby available adsorption sites resulting in a coverage-independent adsorption probability. Additionally, the high values of sticking coefficients indicate that there is no significant barrier for the adsorption. Therefore, the desorption energies measured by TPD (see below) are equivalent to binding and adsorption energies for these adsorbates.

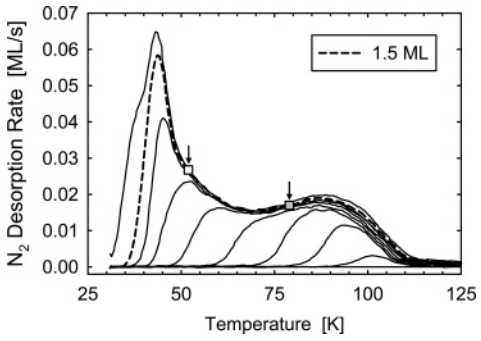

Figure 3. N_2 TPD spectra for various initial N_2 coverages (0, 0.03, 0.20, 0.42, 0.61, 0.82, 1.07, 1.29, 1.50, 1.79) on TiO_2(110). N_2 was adsorbed at 32 K, and the sample was heated linearly at a rate of 1 K/s. The squares are placed on the 1.5 ML (dashed) curve at temperatures where 1 ML (open square) and 0.5 ML (gray square) remain.

The nearly coverage-independent behavior observed on TiO_2(110) is in marked contrast to the behavior observed for CO,[7] N_2,[32] O_2,[32] Ar,[31] and CH_4[31] on MgO(100) where the initial sticking coefficient is low (0.05−0.45) and increases linearly to near unity with increasing coverage for all of these molecules. As shown previously, this linear dependence arises from inefficient energy transfer to the bare MgO(100) surface at low coverage and facile energy transfer with the adsorbate-covered MgO(100) surface.[31] The origin of the differences in the adsorption dynamics observed on TiO_2(110) and MgO(100) is unclear. We speculate that the energy transfer to bare TiO_2(110) is more efficient than to bare MgO(100). Additional experiments beyond the scope of this paper are required to fully resolve this issue.

III.B. Temperature-Programmed Desorption. For selected coverages, defined as indicated above, Figure 3 shows N_2 TPD spectra on TiO_2(110). There are three distinct coverage regions: At low N_2 coverages ($\theta \leq 0.5$ ML), the TPD exhibits a single peak whose maximum shifts from 105 to 90 K as θ increases. At intermediate coverages (0.5−1.0 ML), there is a dramatic shift of intensity to lower temperature (90−45 K). Above $\theta \cong 1$ ML, an additional low-temperature peak develops at ∼43 K. This peak saturates at $\theta \cong 1.5$ ML (dashed curve). Open and gray squares (marked with arrows) represent points on the dashed desorption trace where desorption has reduced the remaining coverage to ∼1.0 and 0.5 ML, respectively. With increasing dose, only slightly higher coverages can be obtained at our sample base temperature (32 K) and N_2 beam flux (1×10^{14} $N_2/s \cdot cm^2$). This added coverage appears as a low-temperature shoulder on the 43 K TPD peak. Our previous study of N_2 on MgO(100) at a lower base temperature (∼22 K) showed a second layer desorption peak in the same (30−40 K) temperature range.[33] Therefore, we argue that the TiO_2(110) surface sites are fully saturated at 1.5 ML and the low-temperature shoulder corresponds to N_2 in the second layer. This argument is supported by theoretical studies of N_2 physisorption on TiO_2(110) as discussed below.[18]

Schematic views (Figure 4) illustrate the plausible configurations of N_2 adsorbed on TiO_2(110) at different coverages. The clean surface (Figure 4a) is composed of alternating rows of five-coordinated Ti^{4+} ions (small dark-gray circles) and BBO ions (large white circles) running along the [001] direction. The

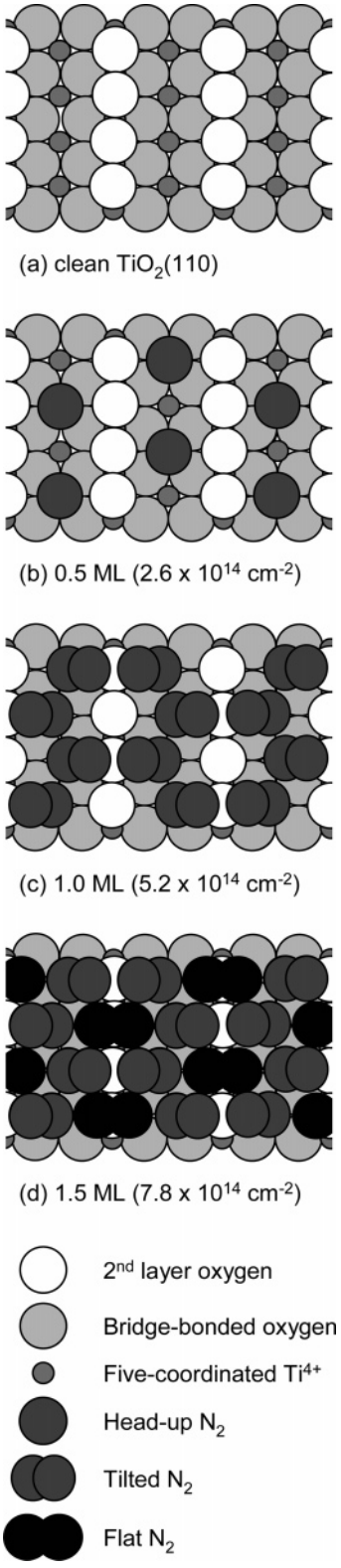

Figure 4. Schematic illustration of N_2 adsorption geometry on TiO_2(110) as a function of coverage: (a) clean TiO_2(110), (b) 0.5 ML of N_2 (2.6×10^{14} N_2/cm^2), (c) 1.0 ML of N_2 (5.2×10^{14} N_2/cm^2), and (d) 1.5 ML of N_2 (7.8×10^{14} N_2/cm^2). The adsorbate structures are based on theoretical calculations by Rittner and co-workers (refs 16 and 18).

distances between neighboring Ti^{4+} sites and/or neighboring BBO sites along the [001] and [1$\bar{1}$0] directions are 2.95 and 6.5 Å, respectively.[1]

A schematic illustration of a plausible structure for $\theta = 0.5$ ML is shown in Figure 4b. On the basis of calculations, an isolated N_2 molecule binds directly to a Ti^{4+} ion in an end-on configuration with the N≡N bond aligned perpendicular to the surface plane.[16] In Figure 4b, N_2 molecules are separated by an empty Ti^{4+} site along a given row, i.e., $\theta = 0.5$ ML, and staggered with respect to each other in adjacent rows. This 2×2 structure minimizes the repulsion between neighboring N_2 molecules. Whether the N_2 forms such an ordered overlayer at 0.5 ML is uncertain, and further studies are required to address this issue. As clearly evident from the TPD spectra in Figure 3, a small but observable shift to lower temperature with increasing coverage is observed even for N_2 coverages less than 0.5 ML. This small shift is indicative of mild adsorbate−adsorbate repulsion consistent with the adsorption configuration of Figure 4b that minimizes the net repulsion.

Increasing the N_2 coverage beyond 0.5 ML requires some fraction of the N_2 molecules to have neighbors bound to adjacent Ti^{4+} sites, resulting in stronger adsorbate−adsorbate repulsion. This repulsion accounts for the dramatic shift to lower temperature (90−45 K) observed in the TPD spectra (see Figure 3) as the coverage is increased from 0.5 to 1.0 ML. The N_2 adsorption structure for $\theta = 1.0$ ML, Figure 4c, is based on the KMC simulations by Rittner et al.[18] In this structure, repulsion causes adjacent N_2 molecules to tilt away from each other and adopt a zigzag chain configuration along a given row of Ti^{4+} ions. Depending on the arrangement of neighboring N_2 chains, both in-phase and out-of-phase configurations are found in the KMC simulations.[18] Three out-of-phase chains are shown in Figure 4c.

Adsorption on the BBO rows accounts for N_2 coverage above 1 ML. These sites bind N_2 significantly less tightly than the Ti^{4+} sites and account for the low-temperature peak (~43 K) in the TPD spectra (Figure 3). It is interesting to note that this peak saturates for $^1/_2$ N_2 per BBO site, consistent with KMC simulations.[18] To accommodate the additional 0.5 ML of N_2 molecules bound to the BBO sites, the 1.0 ML of N_2 bound to the Ti^{4+} sites arrange themselves in the out-of-phase chain configuration. This out-of-phase arrangement of tilted N_2 chains blocks every other BBO site, Figure 4c, leaving only 0.5 ML of open BBO sites. The N_2 molecules maximize their attractive interactions (surface and neighboring N_2) with the N≡N axis perpendicular to and directly over the BBO rows, Figure 4d.

With the use of an inversion procedure,[7,34,35] the N_2 TPD spectra (Figure 3) can be analyzed to extract the coverage dependence of the desorption energy, $E_d(\theta)$. Briefly, by integration of a TPD trace, instantaneous coverages are determined for each temperature along that trace. The resulting coverage−temperature data sets are used to calculate a coverage-dependent desorption energy from a first-order Polanyi−Wigner equation:[36]

$$-\frac{d\theta}{dt} = \nu(\theta)\,\theta \exp[-E_d(\theta)/RT] \qquad (1)$$

Here, θ is the instantaneous adsorbate coverage, t the time, ν the preexponential factor for desorption, E_d the desorption activation energy, R the gas constant, and T the temperature. T and t are related by $dT/dt = \beta$, where β is the heating rate. To invert the Polanyi−Wigner equation, we assume ν is independent of θ and solve eq 1 for $E_d(\theta)$ at each point along a desorption trace. Then $E_d(\theta)$ is used to simulate, by numerical integration of eq 1, a set of TPD spectra for comparison with measured spectra, i.e., various initial coverages and a linear heating rate of 1 K/s.

The optimum value of ν is determined by treating it as a variational parameter and minimizing the error between the

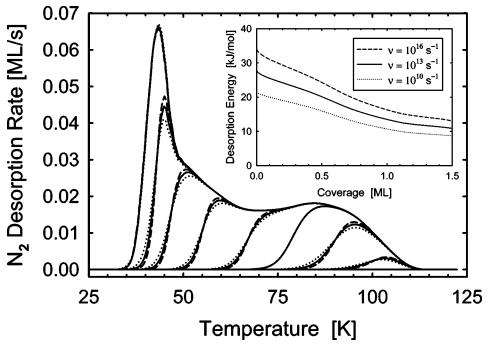

Figure 5. Three sets of simulated N_2 TPD spectra for various initial N_2 coverages ($0 \leq \theta \leq 1.5$ ML). The corresponding sets of preexponential factors and coverage-dependent desorption energies used in the simulations are shown in the inset.

experimentally observed and numerically simulated TPD spectra.[34] This procedure works well when E_d is a weakly varying function of coverage.[7,34,35] Unfortunately for N_2 on TiO_2(110), E_d varies significantly with θ due the presence of strong repulsive adsorbate−adsorbate interactions as well as the presence of different adsorption sites. Consequently varying ν over a relatively broad range (10^{10} to 10^{16} s^{-1}) has little impact on the simulated TPD spectra. To illustrate, Figure 5 shows three sets of TPD spectra simulated using values of ν equal to 10^{10} (dotted lines), 10^{13} (solid lines), and 10^{16} s^{-1} (dashed lines) and the corresponding E_d versus θ dependence (inset of Figure 5) determined by the inversion method. For each prefactor ν, $E(\theta)$ is obtained by inverting the experimental 1.5 ML TPD spectrum (dashed line in Figure 3). As evident from eq 1, an increase (decrease) in the value of ν has to be accompanied by an increase (decrease) in the value of $E(\theta)$ to keep the desorption rate constant at a particular coverage, θ, and temperature, T. From the comparison of the TPD spectra obtained using three different sets of kinetic parameters, ν and $E_d(\theta)$, it is clear that even relatively large variations in ν lead only to small differences in the simulated set of TPD spectra. As illustrated in Figure 5, the leading edge is the only region of a given TPD spectrum that is sensitive to the choice of ν. When the intensity of a given spectrum approaches the common envelope of the saturation spectrum ($\theta = 1.5$ ML) the desorption rate becomes insensitive to the value of ν. This insensitivity leads to a relatively large (±25%) uncertainty in the absolute value of E_d for a given coverage.

Turning to the adsorption and desorption of O_2 (Figure 6) and CO (Figure 7) from TiO_2(110), we note many common features with N_2 (Figure 3). The apparent noise in the CO spectra

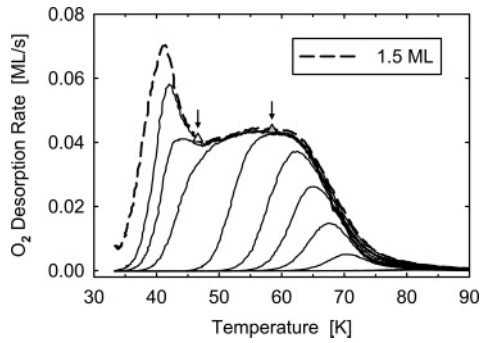

Figure 6. O_2 TPD spectra for various initial O_2 coverages (0, 0.04, 0.13, 0.25, 0.42, 0.69, 1.01, 1.16, 1.31, 1.50) on TiO_2(110). O_2 was adsorbed at 32 K, and the sample was heated linearly at a rate of 1 K/s. The triangles are placed on the 1.5 ML (dashed) curve at temperatures where 1 ML (open triangle) and 0.5 ML (gray triangle) remain.

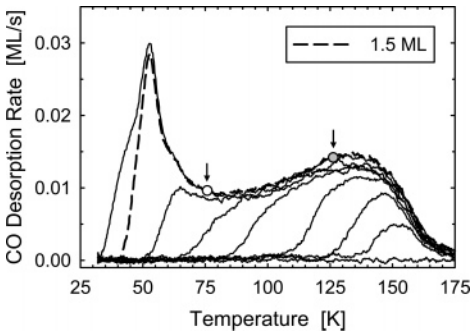

Figure 7. CO TPD spectra for various initial N_2 coverages (0, 0.18, 0.31, 0.50, 0.75, 0.84, 1.06, 1.50, 1.63) on TiO_2(110). CO was adsorbed at 32 K, and the sample was heated linearly at a rate of 1 K/s. The circles are placed on the 1.5 ML (dashed) curve at temperatures where 1 ML (open circle) and 0.5 ML (gray circle) remain.

arises from the fact that data were obtained with a deteriorating electron multiplier near the end of its life span. The higher quality O_2 and N_2 data were obtained with a fully functioning multiplier. The TPD profiles change with coverage in the same qualitative fashion, and the sticking coefficient varies, at most, weakly with coverage indicating a precursor-mediated adsorption mechanism for all three monolayers. Previous studies employing transition state theory suggest that desorption via a mobile precursor gives rise to a desorption prefactor of $\sim 10^{13}$ s^{-1} due to similar values of the adsorbate and transition state partition functions.[37] Based on these theoretical arguments, we employ a prefactor of 10^{13} s^{-1} in our kinetic analysis of the O_2 and CO TPD spectra.

At low coverages ($\theta < 0.5$ ML), the O_2 TPD peak shifts from 70 to 60 K while for CO it shifts from 155 to 135 K. At intermediate coverages (0.5−1.0 ML), the TPD intensity shifts dramatically to lower temperature from 60 to 40 K for O_2 and 135 to 60 K for CO. As for N_2, 1 ML is 5.2×10^{14} cm^{-2}, sufficient to saturate the Ti^{4+} sites. Above $\theta \cong 1$ ML, an additional low-temperature peak develops at ∼41 K for O_2 and at ∼52 K for CO. This peak saturates at $\theta \cong 1.5$ ML (dashed lined of Figures 6 and 7). As for the N_2 spectra, open and gray symbols (marked with arrows) represent points on the dashed desorption traces where desorption has reduced the remaining coverage to ∼1.0 and 0.5 ML, respectively. By analogy with N_2, this low-temperature peak corresponds to adsorption of ∼0.5 ML on top of the BBO sites on TiO_2(110).

It should be noted that no O_2 desorption was observed at high temperatures (∼410 K) characteristic of reduced TiO_2(110).[8,9] The absence of this high-temperature O_2 desorption feature provides further support for the close-to-stoichiometric nature of the TiO_2(110) surfaces employed in this study.

Prior studies of CO adsorption on TiO_2(110) by Linsebigler et al.[5] were conducted at a sample temperature, 105 K, too high to fully saturate the surface sites. Thus, a single CO TPD peak, saturated at 2.1×10^{14} CO/cm^2 ($\theta = 0.4$ ML), was observed. In excellent agreement with the data of Figure 7 (above 105 K), this peak showed a slight shift to lower temperature with increasing coverage. Theoretical calculations have shown that at these low coverages, CO binds to the Ti^{4+} sites in an upright C-end down configuration with neighboring CO molecules spaced by at least one empty Ti^{4+} site.[10−14] While this arrangement minimizes the repulsive interactions between the neighboring CO molecules, the observed TPD shift indicates that the repulsive interactions, presumably dipole-dominated, between CO molecules separated by bare Ti^{4+} sites are still significant.

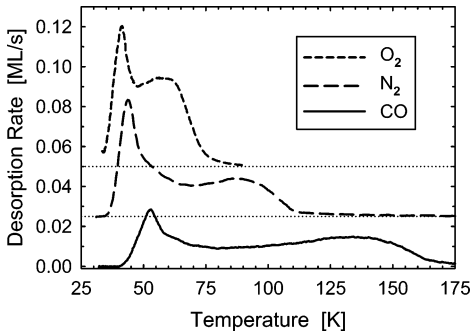

Figure 8. TPD spectra for 1.5 ML of N_2, O_2, and CO adsorbed on TiO_2(110) at 32 K. All spectra are acquired with a sample heating rate of 1 K/s.

TABLE 1: Polarizabilities, α, Dipole Moments, μ, and Quadrupole Moments, Q, for O_2, N_2, and CO Molecules[a]

	α [Å^3]	μ [debye]	Q [10^{-26} esu]
O_2	1.59	0	0.4
N_2	1.74	0	1.5
CO	1.98	0.11	2.0

[a] Ref 38.

To further compare the behavior of O_2, N_2, and CO we plot the 1.5 ML desorption traces in Figure 8. A dramatic increase in the peak desorption temperatures for O_2 (60 K), N_2 (90 K), and CO (135 K) bound on Ti^{4+} ions at $\theta = 0.5$ ML is readily apparent reflecting significant differences in the molecular properties involved in physisorption (Table 1). From O_2 to CO the peak desorption temperature increases more than factor of 2. Since the polarizabilities[38] (Table 1) differ by less than factor of 1.25 ($\alpha_{O_2} = 1.59$, $\alpha_{N_2} = 1.74$, $\alpha_{CO} = 1.98$ Å^3), a significant contribution to the CO and N_2 binding is likely to be electrostatic and associated with the dipole and quadrupole moments in the case of CO and N_2, respectively. At higher coverages (0.5−1.0 ML), the presence of aligned dipole (CO) and quadrupole (N_2) moments will lead to repulsive interactions and account for the dramatic shift of the TPD leading edges to lower temperatures, ∼60 K shift for CO (Figure 7) and ∼40 K shift for N_2 (Figure 3). The smallest shift of ∼20 K is observed for O_2 which has no dipole and the smallest quadrupole moment of these three molecules (see Table 1).

The qualitatively similar CO, N_2, and O_2 TPD character is further evidenced in the extracted E_d versus θ dependences for CO, N_2, and O_2 (Figure 9). For each adsorbate, three distinct E_d versus θ sections are observed. These regions can be easily rationalized using the model, based on theory,[16−18] used to describe physisorption of N_2. At low coverages ($\theta < 0.5$ ML), E_d decreases slowly with increasing θ, since the molecules adsorbed on Ti^{4+} are spaced by empty Ti^{4+} sites and the repulsive adsorbate−adsorbate interactions are minimized. For intermediate coverages (0.5−1.0 ML), E_d decreases sharply as the adsorbates fill neighboring Ti^{4+} sites, and their binding energy is lowered due to strong adsorbate−adsorbate repulsion. At high coverages (1.0−1.5 ML) adsorption takes place on BBO sites, and the values of E_d decrease only slightly with increasing θ. The empty (gray) symbols mark coverages of 0.5 ML (1.0 ML) and correspond to the points labeled on the dashed TPD spectra in Figures 3, 6, and 7.

The binding (adsorption) energies extracted for O_2, N_2, and CO on TiO_2(110) (Figure 9) using the preexponential factor of 10^{13} s^{-1} at coverages of 0, 0.5, 1.0, and 1.5 ML are summarized in Table 2. The zero-coverage limit of CO binding energy ($E_d^{CO}(0) = 42$ kJ/mol) determined in our study can be compared with

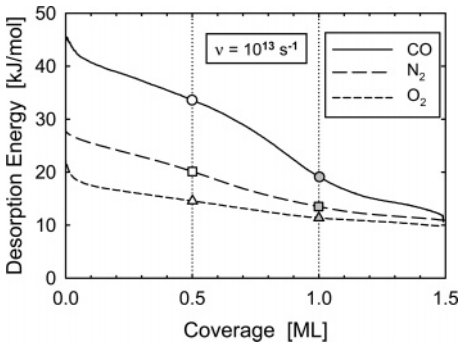

Figure 9. Coverage-dependent desorption energy, $E_d(\theta)$, for CO, N_2, and O_2 obtained from inversion analysis of the experimental TPD spectra shown in Figure 8. First-order desorption, a constant preexponential factor of 1×10^{13} s^{-1}, and a heating rate of 1 K/s are used in the inversion procedure. Circles, squares, and triangles mark positions as in Figures 3, 6, and 7. Note that the extracted energies depend strongly on the value of the prefactor used in the TPD inversion analysis as shown in Figure 5.

TABLE 2: Desorption Energies for O_2, N_2, and CO on TiO_2(110) for Coverages of 0, 0.5, 1.0, and 1.5 ML[a]

	E_d(0 ML) [kJ/mol]	E_d(0.5 ML) [kJ/mol]	E_d(1.0 ML) [kJ/mol]	E_d(1.5 ML) [kJ/mol]
O_2	18	14.5	11.4	9.8
N_2	28	21.0	13.5	10.8
CO	42	33.6	19.1	12.0

[a] Note that the extracted energies depend strongly on the value of the prefactor used in the TPD inversion analysis as shown in Figure 5.

previously published values.[5,6] Using the preexponential factor of 10^{14} s^{-1} Linsebigler et al.[5] obtained $E_d^{CO}(0) = 41.6$ kJ/mol, and Kunat and Burghaus[6] found $E_d^{CO}(0) = 32.3$ kJ/mol. Our value, $E_d^{CO}(0) = 45$ kJ/mol, obtained using $\nu = 10^{14}$ s^{-1}, is in good agreement with the value of Linsebigler et al.[5] but deviates substantially from that of Kunat and Burghaus.[6]

IV. Conclusions

Adsorption and desorption of weakly bound O_2, N_2, and CO were studied on fully oxidized TiO_2(110) at cryogenic temperatures (T as low as 32 K). The sticking coefficients are nearly equal (0.75 ± 0.05) and increase, at most, 10% with increasing coverage, suggesting adsorption via a precursor-mediated mechanism.

Three distinct coverage regions are evident in temperature-programmed desorption (TPD) for all three molecules. Coverage-dependent desorption energies were determined using TPD. The interpretation of the coverage dependence is based on the excellent correlation between our data and the theoretical calculations of Rittner et al. for N_2/TiO_2(110),[16−18] as follows:

(1) At low coverages (0−0.5 ML, (adsorbates/Ti^{4+})), the adsorbates bind to Ti^{4+} ions with unoccupied Ti^{4+} neighbors (see Figure 4b). This arrangement minimizes the variations of the repulsive adsorbate−adsorbate interactions consistent with the observed relatively small temperature shift in the TPD peaks with increasing coverage. The extracted binding energies for O_2, N_2, and CO in the zero-coverage limit are 18, 28, and 42 kJ/mol, respectively, assuming a preexponential factor of 10^{13} s^{-1}.

(2) At intermediate coverages (0.5−1.0 ML), the adsorbates bind to the remaining empty Ti^{4+} sites. Due to the close proximity of adjacent Ti^{4+} (2.95 Å), the adsorbates repel each other and are destabilized. This destabilization results in a significant shift of the TPD spectra to lower temperature with increasing coverage. The most dramatic shift (135−60 K) is

observed for CO, presumably due to the repulsion between aligned dipole moments of the neighboring CO molecules. Simulations by KMC of N_2 adsorption[18] indicate that the repulsive interaction between neighboring N_2 molecules leads to tilting of the N≡N axis away from the surface normal and the formation of zigzag chains along the Ti^{4+} rows as shown in Figure 4c.

(3) At high coverages (1.0−1.5 ML), further adsorption occurs on bridge-bonded oxygen (BBO) sites (see Figure 4d). The TiO_2(110) surface becomes completely saturated at 1.5 ML, when half of the BBO sites are covered. The remaining half are blocked by the tilted adsorbates bound on the Ti^{4+} sites (zigzag chains) as shown in the Figure 4d.

Coverage-dependent binding energies for O_2, N_2, and CO on TiO_2(110) were determined by inversion analysis of experimental TPD spectra. The presence of strong repulsive adsorbate−adsorbate interactions as well as the presence of different adsorption sites did not allow for precise determination of the values of preexponential factors ($10^{13\pm3}$ s^{-1}). A typical value of 10^{13} s^{-1} was used to calculate the desorption energies at coverages of 0, 0.5, 1.0, and 1.5 ML as summarized in Table 2.

Acknowledgment. This work was supported by the U.S. Department of Energy Office of Basic Energy Sciences, Chemical Sciences and Materials Sciences Divisions, and it was performed at the W. R. Wiley Environmental Molecular Science Laboratory, a national scientific user facility sponsored by the Department of Energy's Office of Biological and Environmental Research located at Pacific Northwest National Laboratory. PNNL is operated for the U.S. DOE by Battelle under Contract No. DE-AC06-76RLO 1830. J.M.W. acknowledges support by the U.S. Department of Energy Office of Basic Energy Sciences, Chemical Sciences Division under Grant DE-FG02-03ER15480 to the University of Texas and by the Robert A. Welch Foundation and Center for Materials Chemistry at the University of Texas.

References and Notes

(1) Diebold, U. *Surf. Sci. Rep.* **2003**, *48*, 53.
(2) Stiehl, J. D.; Kim, T. S.; Reeves, C. T.; Meyer, R. J.; Mullins, C. B. *J. Phys. Chem. B* **2004**, *108*, 7917.
(3) Kim, T. S.; Stiehl, J. D.; Reeves, C. T.; Meyer, R. J.; Mullins, C. B. *J. Am. Chem. Soc.* **2003**, *125*, 2018.
(4) Meyer, R.; Lemire, C.; Shaikhutdinov, S. K.; Freund, H.-J. *Gold Bull.* **2004**, *37*, 72.
(5) Linsebigler, A.; Lu, G. Q.; Yates, J. T., Jr. *J. Chem. Phys.* **1995**, *103*, 9438.
(6) Kunat, M.; Burghaus, U. *Surf. Sci.* **2003**, *544*, 170.
(7) Dohnálek, Z.; Kimmel, G. A.; Joyce, S. A.; Ayotte, P.; Smith, R. S.; Kay, B. D. *J. Phys. Chem. B* **2001**, *105*, 3747.
(8) Henderson, M. A.; Epling, W. S.; Perkins, C. L.; Peden, C. H. F.; Diebold, U. *J. Phys. Chem. B* **1999**, *103*, 5328.
(9) Thompson, T. L.; Diwald, O.; Yates, J. T., Jr. *Chem. Phys. Lett.* **2004**, *393*, 28.
(10) Reinhardt, P.; Causa, M.; Marian, C. M.; Hess, B. A. *Phys. Rev. B* **1996**, *54*, 14812.
(11) Pacchioni, G.; Ferrari, A. M.; Bagus, P. S. *Surf. Sci.* **1996**, *350*, 159.
(12) Sorescu, D. C.; Yates, J. T., Jr. *J. Phys. Chem. B* **1998**, *102*, 4556.
(13) Casarin, M.; Maccato, C.; Vittadini, A. *J. Phys. Chem. B* **1998**, *102*, 10745.
(14) Yang, Z. X.; Wu, R. Q.; Zhang, Q. M.; Goodman, D. W. *Phys. Rev. B* **2001**, *63*, 045419.
(15) Calatayud, M.; Markovits, A.; Menetrey, M.; Mguig, B.; Minot, C. *Catal. Today* **2003**, *85*, 125.
(16) Rittner, F.; Fink, R.; Boddenberg, B.; Staemmler, V. *Phys. Rev. B* **1998**, *57*, 4160.
(17) Rittner, F.; Boddenberg, B.; Fink, R. F.; Staemmler, V. *Langmuir* **1999**, *15*, 1449.
(18) Rittner, F.; Boddenberg, B.; Bojan, M. J.; Steele, W. A. *Langmuir* **1999**, *15*, 1456.
(19) De Lara-Castells, M. P.; Krause, J. L. *Chem. Phys. Lett.* **2002**, *354*, 483.
(20) De Lara-Castells, M. P.; Krause, J. L. *J. Chem. Phys.* **2003**, *118*, 5098.
(21) Wu, X. Y.; Selloni, A.; Lazzeri, M.; Nayak, S. K. *Phys. Rev. B* **2003**, *68*, 241402.
(22) Rasmussen, M. D.; Molina, L. M.; Hammer, B. *J. Chem. Phys.* **2004**, *120*, 988.
(23) Schlichting, H.; Menzel, D. *Rev. Sci. Instrum.* **1993**, *64*, 2013.
(24) Kurtz, R.; Stockbauer, R.; Madey, T.; Roman, E.; Desegovia, J. *Surf. Sci.* **1989**, *218*, 178.
(25) Hugenschmidt, M.; Gamble, L.; Campbell, C. *Surf. Sci.* **1994**, *302*, 329.
(26) Henderson, M. *Langmuir* **1996**, *12*, 5093.
(27) Henderson, M. *Surf. Sci.* **1998**, *400*, 203.
(28) White, J.; Szanyi, J.; Henderson, M. *J. Phys. Chem. B* **2003**, *107*, 9029.
(29) Schaub, R.; Thostrup, R.; Lopez, N.; Laegsgaard, E.; Stensgaard, I.; Norskov, J. K.; Besenbacher, F. *Phys. Rev. Lett.* **2001**, *87*, 266104.
(30) King, D. A.; Wells, M. G. *Surf. Sci.* **1972**, *29*, 454.
(31) Dohnálek, Z.; Smith, R. S.; Kay, B. D. *J. Phys. Chem. B* **2002**, *106*, 8360.
(32) Dohnálek, Z.; Kay, B. D. Unpublished work, 2002.
(33) Dohnálek, Z.; Kimmel, G. A.; McCready, D. E.; Young, J. S.; Dohnálková, A.; Smith, R. S.; Kay, B. D. *J. Phys. Chem. B* **2002**, *106*, 3526.
(34) Tait, S. L.; Dohnálek, Z.; Campbell, C. T.; Kay, B. D. *J. Chem. Phys.* **2005**, *122*, 164707.
(35) Tait, S. L.; Dohnálek, Z.; Campbell, C. T.; Kay, B. D. *J. Chem. Phys.* **2005**, *122*, 164708.
(36) de Jong, A. M.; Niemantsverdriet, J. W. *Surf. Sci.* **1990**, *233*, 355.
(37) Zhdanov, V. P. *Elementary Physiochemical Processes on Solid Surfaces*; Plenum Press: New York, 1991.
(38) Gray, C. G.; Gubbins, K. G. *Theory of Molecular Fluids*; Clarendon Press: Oxford, 1984; Vol. 1 Fundamentals.